How to cite: *Angew. Chem. Int. Ed.* **2025**, *64*, e202414583
doi.org/10.1002/anie.202414583

On-Surface Synthesis

Coronene-Based 2D Networks by On-Surface Skeletal Rearrangement of Sumanene Precursors

Elena Pérez-Elvira, Ana Barragán, Aurelio Gallardo, José Santos, Cristina Martín-Fuentes, Koen Lauwaet, José M. Gallego, Rodolfo Miranda, Hidehiro Sakurai, José I. Urgel, Jonas Björk,* Nazario Martín,* and David Écija**

Abstract: The design of novel low-dimensional carbon materials is at the forefront of modern chemistry. Recently, on-surface covalent synthesis has emerged as a powerful strategy to synthesize previously precluded compounds and polymers. Here, we report a scanning probe microscopy study, complemented by theoretical calculations, on the sequential skeletal rearrangement of sumanene-based precursors into a coronene-based organometallic network by stepwise intra- and inter-molecular reactions on Au(111). Interestingly, upon higher annealing, the formed organometallic networks evolve into two-dimensional coronene-based covalently linked patches through intermolecular homocoupling reactions. A new reaction mechanism is proposed based on the role of C–Au–C motifs to promote two stepwise carbon-carbon couplings to form cyclobutadiene bridges. Our results pave avenues for the conversion of molecular precursors on surfaces, affording the design of unexplored two-dimensional organometallic and covalent materials.

Introduction

Two-dimensional (2D) materials have emerged as a cutting-edge research area in the field of materials science, offering a unique set of properties and potential applications that are unattainable in their bulk counterparts. Since the pioneering discovery of graphene, a significant portion of research efforts have been dedicated to inorganic materials. However, recent trends indicate alternative focus on the synthesis of 2D metal-organic, organometallic, and covalent nanomaterials. This growing interest is driven by their extensive design variability, potential biocompatibility, environmental benignity, flexibility, ultra-thin structure, cost-effective fabrication methods, and a compelling array of optical, electronic, magnetic, topological, sensing, and catalytic properties.[1–3]

Within this frame, on-surface synthesis has been revealed as a powerful strategy to synthesize defect-free low-dimensional organic and organometallic materials, frequently introducing unique reactions while, at the same time, allowing the capabilities of scanning probe microscopies for structural, electronic and magnetic characterization at the atomic scale.[4–7] Seminal examples include the synthesis on metallic surfaces of nanographenes,[8–13] the formation of 1D nanowires,[5,14–17] the engineering of quasi-1D conjugated ladder polymers (graphene nanoribbons),[18–21] or even the atomically precise production of 2D covalent networks.[22–24]

Particularly relevant to the on-surface synthesis field is how to exploit intramolecular reactions to engineer functional organic molecules.[7] Among them, rearrangement reactions have proven to be significant in chemical research, serving as an excellent alternative for inducing the formation of novel nanostructures that are otherwise inaccessible.

[*] E. Pérez-Elvira, Dr. A. Barragán, Dr. A. Gallardo, Dr. C. Martín-Fuentes, Dr. K. Lauwaet, Prof. R. Miranda, Dr. J. I. Urgel, Prof. N. Martín, Prof. D. Écija
IMDEA Nanoscience, C/ Faraday 9, Campus de Cantoblanco, 28049 Madrid, Spain
E-mail: jose-ignacio.urgel@imdea.org
david.ecija@imdea.org

Dr. J. Santos, Prof. N. Martín
Departamento de Química Orgánica, Facultad de Ciencias Químicas, Universidad Complutense
E-mail: nazmar@ucm.es

Dr. J. M. Gallego
Instituto de Ciencia de Materiales de Madrid (ICMM), CSIC, Cantoblanco, 28049 Madrid, Spain

Dr. J. I. Urgel, Prof. D. Écija
Unidad de Nanomateriales Avanzados, IMDEA Nanoscience, Unidad asociada al CSIC por el ICMM, 28049 Madrid, Spain

Prof. H. Sakurai
Division of Applied Chemistry, Graduate School of Engineering, Osaka University, 2-1 Yamadaoka, Suita, Osaka 565-0871, Japan

Prof. J. Björk
Materials Design Division, Department of Physics, Chemistry, and Biology (IFM), Linköping University, SE-581 83 Linköping, Sweden
E-mail: jonas.bjork@liu.se

Only recently a few skeletal rearrangement reactions induced by atomic manipulation[25–30] or via intramolecular thermal rearrangement[13,31–38] have been studied on surfaces at the single-molecule level. Consequently, further investigations into these types of chemical reactions are essential to gain deeper molecular mechanistic insights, while affording novel chemical products.

Therefore, inspired by our recent discovery of intramolecular rearrangements of acene and indenofluorene derivatives functionalized with carbon *gem*-dibromoalkene functional groups ($=CBr_2$) upon annealing on a Au(111) substrate,[39] here we report the synthesis and on-surface reactivity of precursor **1**, which is a sumanene derivative, i.e. iconic bowl-shaped [60]fullerene fragment,[40] endowed with three $=CBr_2$ groups, each one of them placed at the apex of a five-membered ring, to steer intramolecular rearrangements by thermal stimuli. It is worth mentioning that the study of fullerene fragments on surfaces, also known as buckybowls, have attracted significant interest in view of their peculiar structure, electronic properties and rich metal coordination chemistry, serving as building blocks for novel nanostructures with prospects for organic electronics.[41–45]

Our comprehensive scanning tunneling and non-contact atomic force microscopy (STM / nc-AFM) studies under ultra-high vacuum (UHV) conditions, complemented by density functional theory (DFT) computations, reveal that the deposition of a submonolayer coverage of sumanene derivative (**1**) on a pristine Au(111) substrate held at room temperature (RT) gives rise to a supramolecular self-assembly based on two distinct adsorption geometries: concave and convex (*phase α*). Further annealing induces competing reactions: i) full debromination and homocoupling resulting in disordered patches, and ii) intramolecular rearrangements. Notably, by repeating such deposition protocol, but this time holding the sample at 150 °C, there is a controlled transformation of the sumanene moieties into coronene ones, thanks to a triply intramolecular rearrangement. Such backbones interact supramolecularly affording an organometallic lattice (*phase β*) based on two-fold C–Au–C bonds. A subsequent annealing step induces the formation of 2D covalent porous patches consisting in coronene moieties bridged by cyclobutadiene rings (*phase γ*).

Our findings offer novel strategies for the synthesis of organometallic and covalent low-dimensional nanoarchitectures, by exploiting the intramolecular transformation of molecular precursors and their ulterior intermolecular reactivity.

Results and Discussion

Precursor **1** was synthesized following the procedure described in the Supporting Information (see Figures S1–S3 for infrared and high-resolution mass spectroscopy), to functionalize a sumanene backbone with three $=CBr_2$ moieties. Recently, gem-dibromides were found to be versatile for the on-surface synthesis of carbon nanomaterials.[14–17,21,39,46–49] In particular, it has been reported that the 1,1-dibromo-vinylene functional group can steer polymerization when the precursor species are deposited at RT and subsequently annealed,[14–17,21,47,48] or directly afford intramolecular rearrangement when the precursor is adsorbed on a hot substrate.[39] To elucidate the dominant reaction pathways on Au(111) for the sumanene derivative bestowing three $=CBr_2$ groups, we inspected both scenarios.

The deposition of a submonolayer coverage of **1** on Au(111) held at RT under UHV conditions gives rise to extended self-assembled molecular islands (cf. Figure 1a). An important aspect to take into account at this stage is the three-dimensional shape of the molecular precursor.[40] In fact, two distinct molecular adsorption geometries are detected, stemming from the bowl-shaped conformation of sumanene.[44,50] One species faces the central six-membered ring towards the surface (concave shape, termed bowl-down, cf. Figure 1b–d), and the other one displays the $=CBr_2$

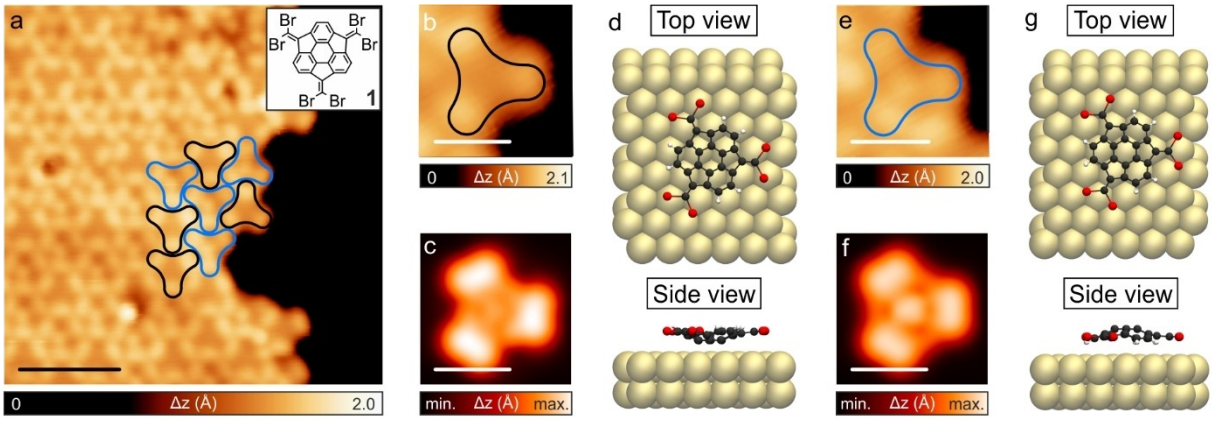

Figure 1. Phase α: Self-assembly of **1** on Au(111). a) Large-scale STM image showing the coexistence of two different adsorption geometries, which feature concave (convex) shapes with $=CBr_2$ moieties pointing upwards (downwards), highlighted in black (blue), respectively. The inset shows the chemical sketch of the molecular precursor **1**. $V_b = 0.5$ V, $I_t = 50$ pA. Scale bar: 3 nm. b), e) STM images of the bowl-down and bowl-up species, respectively. $V_b = -0.5$ V, $I_t = 50$ pA, scale bar: 1 nm. c), f) Simulated STM images of panels (b) and (e). Scale bar: 1 nm. d), g) Top view (upper panel) and side view (lower panel) of the adsorption geometry simulated by DFT of the concave and the convex species, respectively.

moieties pointing downwards and a bright protrusion in the center (assigned to convex shape, named bowl-up, cf. Figure 1e–g). Both of them statistically occur in the same ratio, presenting a very similar adsorption energy with less than 15 meV of difference (see Figure S4). Such adsorption behavior has been previously encountered for pristine sumanene on metals.[44,50] Regardless of the adsorption geometry, the precursors are engaged in a one-layer thick two-dimensional architecture to be termed *phase α*, presumably based on Br···H interactions (see Figure S5). No sign of three-dimensional growth is detected. The match between the experimental visualization of the species and the theoretical simulations is excellent (cf. Figures 1b,c for bowl-down and Figures 1e,f for bowl-up conformations, respectively), ratifying our rationalization.

Annealing at 150 °C results in the formation of irregular covalently linked networks, in which some species have suffered an irregular internal rearrangement, while others are covalently linked displaying a hexagonal pattern with very short-range order (Figure S6). Thus, deposition at RT followed by annealing turns out to be an unsuccessful approach to engineer regular two-dimensional covalent networks.

Alternatively, we deposited a submonolayer coverage of **1** on Au(111) held at 150 °C, which results in a drastically distinct scenario (see reaction sketch in Figure 2a). The surface is now covered by a 2D periodic hexagonal porous network extending over dozens of nm (cf. Figure 2b and Figure S7), to be termed *phase β*. High-resolution constant-current STM imaging reveals that the molecular species display a three-fold symmetry. They are connected to adjacent monomers at their sides by three protrusions, a circular central one and two elongated lateral ones.

To elucidate the nature of the molecular backbones and the supramolecular architecture, constant-height STM (cf. Figure 2c) and constant-height frequency-shift nc-AFM images (cf. Figures 2e–g) were acquired with a CO-functionalized tip.[51,52] The sumanene backbone of the precursor has

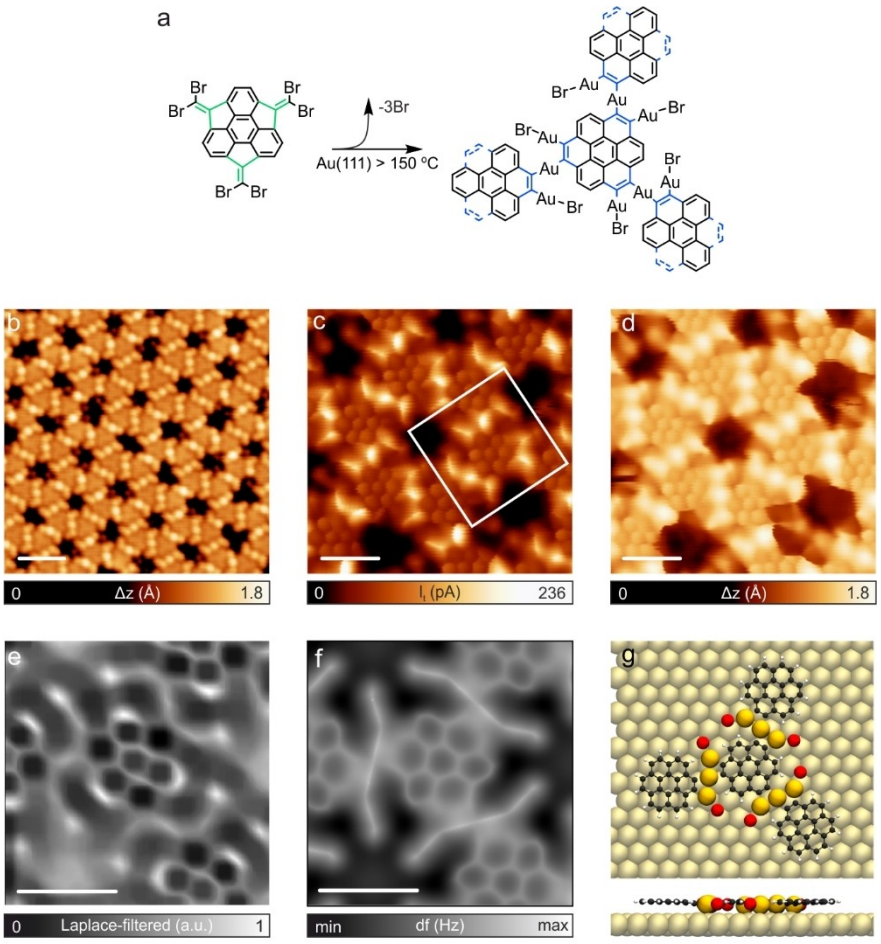

Figure 2. Phase β: On-surface synthesis of the organometallic network on Au(111). a) Chemical sketch of the on-surface chemical reaction pathway when depositing precursor **1** on an Au(111) substrate kept at 150 °C, inducing an intramolecular rearrangement of sumanene-based precursors into coronene ones. b) Large-scale STM image of *phase β*. $V_b = 5$ mV, $I_t = 50$ pA. Scale bar: 2 nm. c) Constant-height high-resolution STM image of an organometallic hexamer acquired with a CO-functionalized tip. $V_b = 50$ mV, $I_t = 50$ pA. Scale bar: 1 nm. d) Detailed constant-current STM image. $V_b = 50$ mV, $I_t = 50$ pA. Scale bar: 8 Å. e) Laplace-filtered constant-height frequency-shift nc-AFM image of the coronene unit indicated by a white square in panel (c), and its three connections to adjacent monomers acquired with a CO-functionalized tip. Z offset: 115 pm above STM set point (5 mV, 50 pA). Scale bar: 1 nm. f) Calculated frequency-shift nc-AFM image of panel (e). g) Calculated structural model of (e).

clearly undergone a three-fold ring expansion, yielding a flat coronene (also known as superbenzene) moiety.[53–56] Importantly, a terminal carbon from the monomer is connected to the one from an adjacent species, tentatively through a two-fold C–Au–C bond, which is visualized as a bright protrusion in STM and as a straight line in nc-AFM.

Each coronene species is then interacting through organometallic C–Au–C bonds with three adjacent species in a chiral fashion, as summarized in the model (cf. Figure 2a). Such rationalization is corroborated by the excellent agreement between the experimental and the calculated nc-AFM images (cf. Figures 2e,f,g). Importantly, each coronene species still preserves three C-Au-Br moieties, which are observed as elongated protrusions in STM and as straight lines directing to the pore in nc-AFM images (cf. Figure S8).

DFT calculations show that the ring rearrangement of a five-membered to a six-membered moiety within a sumanene backbone has an activation energy of merely 0.25 eV (cf. Figure S9). Considering that the molecular precursor stays intact at room temperature, in combination with the fact that debromination barriers[14,57] have been calculated to be significantly higher than this value, it is fair to assume that the debromination is the rate-limiting step for the overall sumanene to coronene expansion (cf. Figure S9 and discussion therein).

Subsequent annealing of *phase β* at 225 °C induces the formation of a new nanoarchitecture, to be termed *phase γ* (cf. Figure 3a and Figure S7), which may also be directly obtained from **1** when deposited on an Au(111) substrate held at 225 °C. High-resolution STM and nc-AFM images and comparison to simulated ones allow us to discern the chemical structure of *phase γ*. It comprises periodic patches based on coronene backbones which are connected in a three-fold fashion to adjacent species by cyclobutadiene rings (cf. Figures 3b–f and Figure S10).

A pore made up of six coronene monomers is displayed in Figure 3b, justifying our chemical rationalization in Figure 3c. Further insights are provided by a monomer and its three cyclobutadiene connections. The DFT simulation of such a structure reveals a flat adsorption, corroborated by nc-AFM imaging (cf. Figure 3e). The cyclobutadiene bridges are distinguished and the overall patch agrees well with the simulation (cf. Figure 3f) and the proposed rationalization (cf. Figure 3g). Importantly, the bond length analysis of *phase γ* based on DFT calculations is in agreement with our interpretation of the bridge as cyclobutadiene, as illustrated in the calculated structural models in Figure 3d and 3h, and in Figure S10. The electronic structure is probed by scanning tunneling spectroscopy revealing a band gap of around 0.8 eV (cf. Figure S11).

To investigate the reaction mechanism driving the transformation of *phase β* into *γ*, we performed further DFT-based calculations. For computational feasibility we chose an initial *phase β* system that consists of two monomers featuring an organometallic environment as depicted in Figure 4, i.e. we only focused on the formation of one cyclobutadiene bridge. Then, we proposed two different reaction pathways. Mechanism 1 is the direct formation of covalent bonds between the molecules after the removal of the Au adatoms in a two stepwise fashion (cf. Figure 4). The alternative pathway (mechanism 2, cf. Figure S12) is moti-

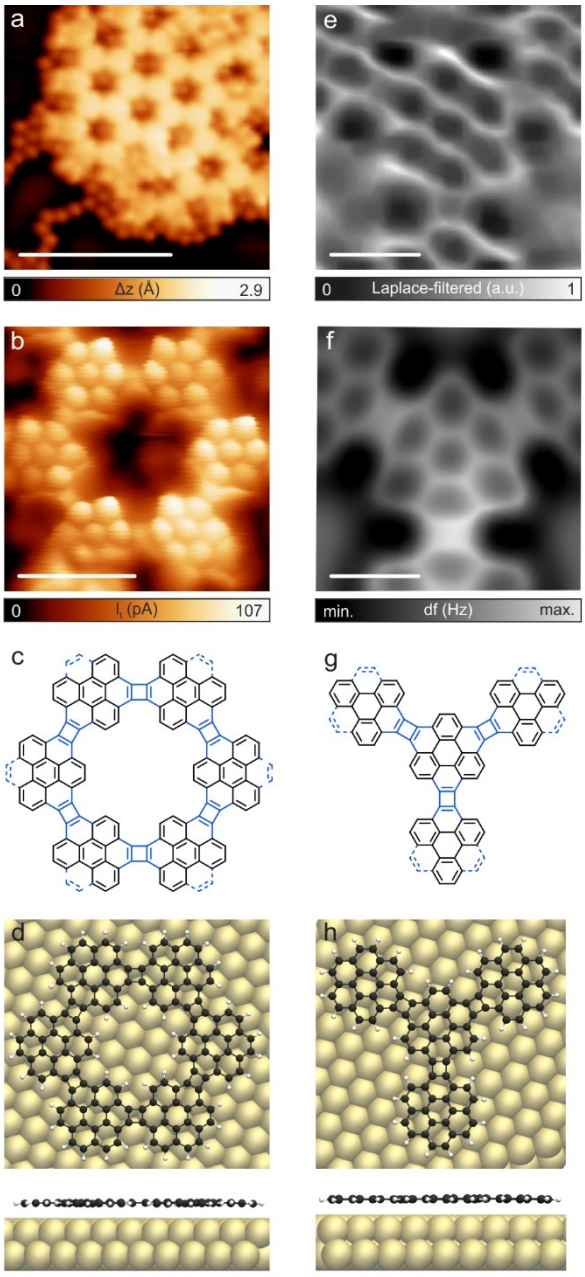

Figure 3. Phase γ: On-surface synthesis of cyclobutadiene-linked coronene-based two-dimensional network on Au(111). a) Large-scale STM image after deposition of **1** on a Au(111) substrate kept at 225 °C. $V_b = -1$ V, $I_t = 50$ pA. Scale bar: 5 nm. b) Constant-height high-resolution STM image, acquired with a CO-functionalized tip, of a patch of *phase γ*. $V_b = 5$ mV, $I_t = 50$ pA. Scale bar: 1 nm. c) and d) Chemical sketch and calculated structural model of (b). e) Laplace-filtered constant-height frequency-shift nc-AFM image, acquired with a CO-functionalized tip, of a coronene unit bonded to three adjacent monomers by cyclobutadiene moieties. Z offset 60 pm above STM set point (5 mV, 50 pA). Scale bar: 0.5 nm. f) Calculated frequency-shift nc-AFM image of (d). g) and h) Chemical sketch and calculated structural model of (e).

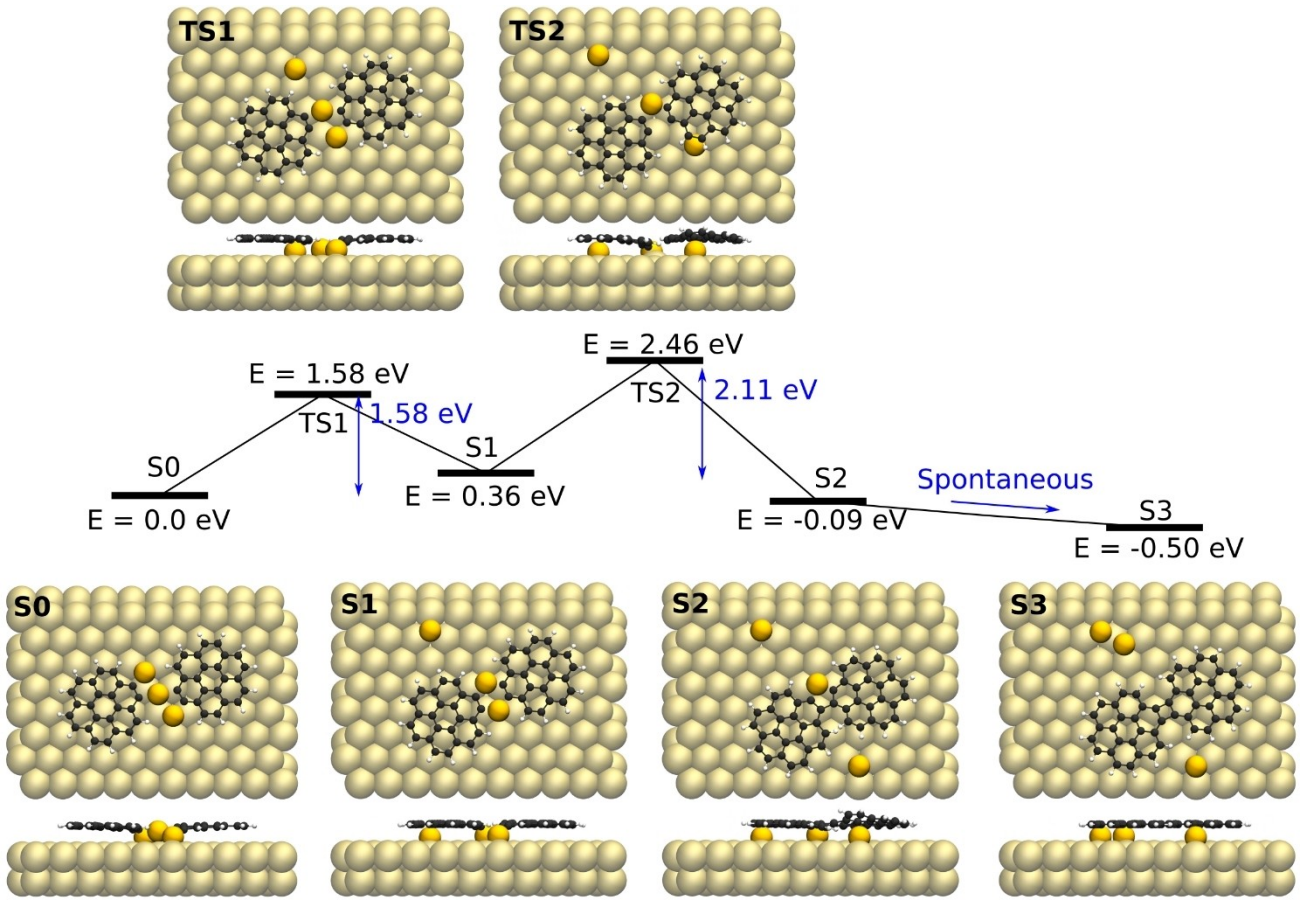

Figure 4. DFT-calculated pathway for transforming *phase* β into *phase* γ. Total energy profile together with top and side views of local minima (**S0**–**S4**, bottom row) and transition states (**TS1** and **TS2**, upper row) of the reaction.

vated by recent literature about the [2+2] cycloaddition[58–61] of hexabromotriphenylene species (HBTP) on Ag(111).[61] In such findings, the adsorption of HBTP species on Ag(111) and subsequent annealing gives rise to the formation of an organometallic phase. Further annealing afforded the expression of covalent patches, driven by the elimination of Ag adatoms from the organometallic nodes and ulterior formal [2+2] cycloaddition.

We found the most favorable mechanism to be the stepwise elimination of the three Au adatoms in between the monomers (mechanism 1), which implies two energy barriers of 1.58 eV and 2.11 eV, respectively, and a final barrierless process, reaching a final configuration making the reaction exothermic with an overall energy gain of 0.50 eV. In Figure 4, we show the initial, intermediates, final and transition state configurations of the three stages of the transformation from *phase* β to γ, along with the activation energies associated to each step of the process. In the first step (**S0** to **S1**), the first Au atom is cleaved from the system, and the molecules rotate to adopt the characteristic alignment of *phase* β. In the second step (**S1** to **S2**), one of the C–Au–C links is already replaced by a covalent bond. Finally, the last organometallic link is spontaneously converted in a covalent bond (**S2** to **S3**), reaching the chemical structure of *phase* γ. The alternative reaction pathway (mechanism 2) in which the molecules diffuse after being dissolved from *phase* β to form the covalent link by a formal [2+2] cycloaddition is presented in Figure S12, though being less favorable than mechanism 1. Thus, the transformation of the organometallic *phase* β into the covalent *phase* γ is mediated by two consecutive carbon-carbon couplings through C–Au–C bonds (mechanism 1).

Conclusions

In summary, we report the synthesis and on-surface reactivity of precursor **1**, a sumanene derivative endowed with three $=CBr_2$ groups strategically placed in five-membered rings to facilitate intramolecular skeletal rearrangements upon thermal stimuli. Our scanning probe microscopy studies and DFT simulations reveal that the deposition of a submonolayer coverage of **1** on a pristine Au(111) surface at RT affords the formation of a supramolecular architecture based on a random distribution of bowl-up and bowl-down species (*phase* α). Such scenario changes drastically when the species are deposited on a hot substrate kept at 150 °C, since a triple intramolecular rearrangement is triggered upon deposition, converting the sumanene moieties into coronene units. These coronene

backbones then interact supramolecularly, forming an organometallic lattice (*phase β*) characterized by two-fold C–Au–C bonds. Subsequent annealing to 225 °C, or deposition of sumanene derivative **1** on an Au(111) surface kept at the same temperature, induces the formation of unprecedented 2D covalent porous patches, with four-membered ring units bridging the coronene moieties (*phase γ*). Based on the role of C–Au–C to promote two stepwise carbon-carbon couplings to steer the cyclobutadiene bridges, a new mechanism that differs from formal [2+2] cycloadditions is presented.

Our findings pave avenues for synthesizing organometallic and covalent low-dimensional nanoarchitectures by exploiting the intramolecular transformation of molecular precursors and their subsequent intermolecular reactivity. This work involving two singular organic molecules, namely sumanene and coronene, expands the frontiers of on-surface synthesis, while advancing the less-known chemistry of bowl-shaped π-conjugated compounds.

Supporting Information

The authors have cited additional references within the Supporting Information.

Acknowledgements

We acknowledge to several funding organizations for their financial support. We thank funding from PID2019-108532GB-I00, PID2020-114653RB-I00, PID2022-136961NB-I00, QUIMTRONIC-CM Y2018/NMT-4783 and the '(MAD2D-CM)-IMDEA-Nanociencia' and '(MAD2D-CM)-UCM' projects funded by Comunidad de Madrid, by the Recovery, Transformation and Resilience Plan, and by NextGenerationEU from the European Union. IMDEA Nanociencia is appreciative of support from the "Severo Ochoa" Programme for Centers of Excellence in R&D (CEX2020-001039-S). A.B. and A.G. acknowledge financial support from Juan de la Cierva program (FJC2021-046524-I and JDC2022-048249-I, respectively). J.I.U. acknowledges financial support from MCIU for the Ramón y Cajal program (RYC2022-037352-I). J.B. acknowledges funding from Swedish Government Strategic Research Area in Materials Science on Advanced Functional Materials at Linköping University, Faculty Grant SFO-Mat-LiU 2009-00971. Computations were enabled by resources provided by the National Academic Infrastructure for Supercomputing in Sweden (NAISS), partially funded by the Swedish Research Council through grant agreement no. 2022-06725. H.S. acknowledges funding from JSPS KAKENHI no. JP21H05233.

Conflict of Interest

The authors declare no conflict of interest.

Data Availability Statement

The data that support the findings of this study are available from the corresponding author upon reasonable request.

Keywords: On-surface Synthesis · C60 fragments · Scanning Tunneling Microscopy · Atomic Force Microscopy

[1] A. K. Geim, K. S. Novoselov, *Nat. Mater.* **2007**, *6*, 183–191.
[2] K. S. Novoselov, A. Mishchenko, A. Carvalho, A. H. Castro Neto, *Science* **2016**, *353*, aac9439.
[3] Q. H. Wang, A. Bedoya-Pinto, M. Blei, A. H. Dismukes, A. Hamo, S. Jenkins, M. Koperski, Y. Liu, Q.-C. Sun, E. J. Telford, H. H. Kim, M. Augustin, U. Vool, J.-X. Yin, L. H. Li, A. Falin, C. R. Dean, F. Casanova, R. F. L. Evans, M. Chshiev, A. Mishchenko, C. Petrovic, R. He, L. Zhao, A. W. Tsen, B. D. Gerardot, M. Brotons-Gisbert, Z. Guguchia, X. Roy, S. Tongay, Z. Wang, M. Z. Hasan, J. Wrachtrup, A. Yacoby, A. Fert, S. Parkin, K. S. Novoselov, P. Dai, L. Balicas, E. J. G. Santos, *ACS Nano* **2022**, *16*, 6960–7079.
[4] Q. Shen, H.-Y. Gao, H. Fuchs, *Nano Today* **2017**, *13*, 77–96.
[5] Q. Sun, R. Zhang, J. Qiu, R. Liu, W. Xu, *Adv. Mater.* **2018**, *30*, 1705630.
[6] S. Clair, D. G. de Oteyza, *Chem. Rev.* **2019**, *119*, 4717–4776.
[7] B. Yang, B. Dong, L. Chi, *ACS Nano* **2020**, *14*, 6376–6382.
[8] Y. Gu, Z. Qiu, K. Müllen, *J. Am. Chem. Soc.* **2022**, *144*, 11499–11524.
[9] K. Biswas, J. I. Urgel, M. R. Ajayakumar, J. Ma, A. Sánchez-Grande, S. Edalatmanesh, K. Lauwaet, P. Mutombo, J. M. Gallego, R. Miranda, P. Jelínek, X. Feng, D. Écija, *Angew. Chem. Int. Ed.* **2022**, *n/a*, e202114983.
[10] W. Zeng, J. Wu, *Chem* **2021**, *7*, 358–386.
[11] S. Song, J. Su, M. Telychko, J. Li, G. Li, Y. Li, C. Su, J. Wu, J. Lu, *Chem. Soc. Rev.* **2021**, *50*, 3238–3262.
[12] K. Biswas, D. Soler, S. Mishra, Q. Chen, X. Yao, A. Sánchez-Grande, K. Eimre, P. Mutombo, C. Martín-Fuentes, K. Lauwaet, J. M. Gallego, P. Ruffieux, C. A. Pignedoli, K. Müllen, R. Miranda, J. I. Urgel, A. Narita, R. Fasel, P. Jelínek, D. Écija, *J. Am. Chem. Soc.* **2023**, *145*, 2968–2974.
[13] T. G. Lohr, J. I. Urgel, K. Eimre, J. Liu, M. Di Giovannantonio, S. Mishra, R. Berger, P. Ruffieux, C. A. Pignedoli, R. Fasel, X. Feng, *J. Am. Chem. Soc.* **2020**, *142*, 13565–13572.
[14] A. Sánchez-Grande, B. de la Torre, J. Santos, B. Cirera, K. Lauwaet, T. Chutora, S. Edalatmanesh, P. Mutombo, J. Rosen, R. Zboril, R. Miranda, J. Björk, P. Jelínek, N. Martín, D. Ecija, *Angew. Chem. Int. Ed.* **2019**, *58*, 6559–6563.
[15] B. Cirera, A. Sánchez-Grande, B. d l Torre, J. Santos, S. Edalatmanesh, E. Rodríguez-Sánchez, K. Lauwaet, B. Mallada, R. Zboril, R. Miranda, O. Gröning, P. Jelínek, N. Martín, D. Ecija, *Nat. Nanotechnol.* **2020**, *15*, 437–443.
[16] A. Sánchez-Grande, J. I. Urgel, I. García-Benito, J. Santos, K. Biswas, K. Lauwaet, J. M. Gallego, J. Rosen, R. Miranda, J. Björk, N. Martín, D. Écija, *Adv. Sci.* **2022**, *9*, 2200407.
[17] H. González-Herrero, J. I. Mendieta-Moreno, S. Edalatmanesh, J. Santos, N. Martín, D. Écija, B. de la Torre, P. Jelinek, *Adv. Mater.* **2021**, *33*, 2104495.
[18] J. Cai, P. Ruffieux, R. Jaafar, M. Bieri, T. Braun, S. Blankenburg, M. Muoth, A. P. Seitsonen, M. Saleh, X. Feng, K. Mullen, R. Fasel, *Nature* **2010**, *466*, 470–473.
[19] L. Talirz, P. Ruffieux, R. Fasel, *Adv. Mater.* **2016**, *28*, 6222–6231.
[20] O. Gröning, S. Wang, X. Yao, C. A. Pignedoli, G. Borin Barin, C. Daniels, A. Cupo, V. Meunier, X. Feng, A. Narita, K. Müllen, P. Ruffieux, R. Fasel, *Nature* **2018**, *560*, 209–213.

[21] B. de la Torre, A. Matěj, A. Sánchez-Grande, B. Cirera, B. Mallada, E. Rodríguez-Sánchez, J. Santos, J. I. Mendieta-Moreno, S. Edalatmanesh, K. Lauwaet, M. Otyepka, M. Medveď, Á. Buendía, R. Miranda, N. Martín, P. Jelínek, D. Écija, *Nat. Commun.* **2020**, *11*, 4567.
[22] C. Moreno, M. Vilas-Varela, B. Kretz, A. Garcia-Lekue, M. V. Costache, M. Paradinas, M. Panighel, G. Ceballos, S. O. Valenzuela, D. Peña, A. Mugarza, *Science* **2018**, *360*, 199.
[23] G. Galeotti, F. De Marchi, E. Hamzehpoor, O. MacLean, M. Rajeswara Rao, Y. Chen, L. V. Besteiro, D. Dettmann, L. Ferrari, F. Frezza, P. M. Sheverdyaeva, R. Liu, A. K. Kundu, P. Moras, M. Ebrahimi, M. C. Gallagher, F. Rosei, D. F. Perepichka, G. Contini, *Nat. Mater.* **2020**.
[24] Q. Fan, L. Yan, M. W. Tripp, O. Krejčí, S. Dimosthenous, S. R. Kachel, M. Chen, A. S. Foster, U. Koert, P. Liljeroth, J. M. Gottfried, *Science* **2021**, *372*, 852–856.
[25] B. Schuler, S. Fatayer, F. Mohn, N. Moll, N. Pavliček, G. Meyer, D. Peña, L. Gross, *Nat. Chem.* **2016**, *8*, 220–224.
[26] N. Pavliček, P. Gawel, D. R. Kohn, Z. Majzik, Y. Xiong, G. Meyer, H. L. Anderson, L. Gross, *Nat. Chem.* **2018**, *10*, 853–858.
[27] F. Albrecht, S. Fatayer, I. Pozo, I. Tavernelli, J. Repp, D. Peña, L. Gross, *Science* **2022**, *377*, 298–301.
[28] Y. Gao, F. Albrecht, I. Rončević, I. Ettedgui, P. Kumar, L. M. Scriven, K. E. Christensen, S. Mishra, L. Righetti, M. Rossmannek, I. Tavernelli, H. L. Anderson, L. Gross, *Nature* **2023**, *623*, 977–981.
[29] L. Sun, W. Zheng, W. Gao, F. Kang, M. Zhao, W. Xu, *Nature* **2023**, *623*, 972–976.
[30] F. Albrecht, I. Rončević, Y. Gao, F. Paschke, A. Baiardi, I. Tavernelli, S. Mishra, H. L. Anderson, L. Gross, *Science* **2024**, *384*, 677–682.
[31] L. E. Dinca, C. Fu, J. M. MacLeod, J. Lipton-Duffin, J. L. Brusso, C. E. Szakacs, D. Ma, D. F. Perepichka, F. Rosei, *ACS Nano* **2013**, *7*, 1652–1657.
[32] S. Kawai, V. Haapasilta, B. D. Lindner, K. Tahara, P. Spijker, J. A. Buitendijk, R. Pawlak, T. Meier, Y. Tobe, A. S. Foster, E. Meyer, *Nat. Commun.* **2016**, *7*, 12711.
[33] A. Shiotari, T. Nakae, K. Iwata, S. Mori, T. Okujima, H. Uno, H. Sakaguchi, Y. Sugimoto, *Nat. Commun.* **2017**, *8*, 16089.
[34] A. Riss, S. Wickenburg, P. Gorman, L. Z. Tan, H.-Z. Tsai, D. G. de Oteyza, Y.-C. Chen, A. J. Bradley, M. M. Ugeda, G. Etkin, S. G. Louie, F. R. Fischer, M. F. Crommie, *Nano Lett.* **2014**, *14*, 2251–2255.
[35] A. Riss, A. P. Paz, S. Wickenburg, H.-Z. Tsai, D. G. De Oteyza, A. J. Bradley, M. M. Ugeda, P. Gorman, H. S. Jung, M. F. Crommie, A. Rubio, F. R. Fischer, *Nat. Chem.* **2016**, *8*, 678–683.
[36] D. G. de Oteyza, P. Gorman, Y.-C. Chen, S. Wickenburg, A. Riss, D. J. Mowbray, G. Etkin, Z. Pedramrazi, H.-Z. Tsai, A. Rubio, M. F. Crommie, F. R. Fischer, *Science* **2013**, *340*, 1434–1437.
[37] K. Biswas, Q. Chen, S. Obermann, J. Ma, D. Soler-Polo, J. Melidonie, A. Barragán, A. Sánchez-Grande, K. Lauwaet, J. M. Gallego, R. Miranda, D. Écija, P. Jelínek, X. Feng, J. I. Urgel, *Angew. Chem. Int. Ed.* **2024**, *63*, e202318185.
[38] Q. Chen, M. Di Giovannantonio, K. Eimre, J. I. Urgel, P. Ruffieux, C. A. Pignedoli, K. Müllen, R. Fasel, A. Narita, *Macromol. Chem. Phys.* **2023**, *224*, 2300345.
[39] E. Pérez-Elvira, A. Barragán, Q. Chen, D. Soler-Polo, A. Sánchez-Grande, D. J. Vicent, K. Lauwaet, J. Santos, P. Mutombo, J. I. Mendieta-Moreno, B. de la Torre, J. M. Gallego, R. Miranda, N. Martín, P. Jelínek, J. I. Urgel, D. Écija, *Nat. Synth.* **2023**, *2*, 1159–1170.
[40] H. Sakurai, T. Daiko, T. Hirao, *Science* **2003**, *301*, 1878–1878.
[41] M. Parschau, R. Fasel, K.-H. Ernst, O. Gröning, L. Brandenberger, R. Schillinger, T. Greber, A. P. Seitsonen, Y.-T. Wu, J. S. Siegel, *Angew. Chem. Int. Ed.* **2007**, *46*, 8258–8261.
[42] T. Bauert, L. Zoppi, G. Koller, A. Garcia, K. K. Baldridge, K.-H. Ernst, *J. Phys. Chem. Lett.* **2011**, *2*, 2805–2809.
[43] Q. S. Stöckl, Y.-C. Hsieh, A. Mairena, Y.-T. Wu, K.-H. Ernst, *J. Am. Chem. Soc.* **2016**, *138*, 6111–6114.
[44] S. Fujii, M. Ziatdinov, S. Higashibayashi, H. Sakurai, M. Kiguchi, *J. Am. Chem. Soc.* **2016**, *138*, 12142–12149.
[45] S. Mishra, M. Krzeszewski, C. A. Pignedoli, P. Ruffieux, R. Fasel, D. T. Gryko, *Nat. Commun.* **2018**, *9*, 1714.
[46] Q. Sun, B. V. Tran, L. Cai, H. Ma, X. Yu, C. Yuan, M. Stöhr, W. Xu, *Angew. Chem. Int. Ed.* **2017**, *56*, 12165–12169.
[47] A. Sánchez-Grande, J. I. Urgel, A. Cahlík, J. Santos, S. Edalatmanesh, E. Rodríguez-Sánchez, K. Lauwaet, P. Mutombo, D. Nachtigallová, R. Nieman, H. Lischka, B. de la Torre, R. Miranda, O. Gröning, N. Martín, P. Jelínek, D. Écija, *Angew. Chem. Int. Ed.* **2020**, *59*, 17594–17599.
[48] C. Martín-Fuentes, J. I. Urgel, S. Edalatmanesh, E. Rodríguez-Sánchez, J. Santos, P. Mutombo, K. Biswas, K. Lauwaet, J. M. Gallego, R. Miranda, P. Jelínek, N. Martín, D. Écija, *Chem. Commun.* **2021**, *57*, 7545–7548.
[49] J. I. Urgel, A. Sánchez-Grande, D. J. Vicent, P. Jelínek, N. Martín, D. Écija, *Adv. Mater.* **2024**, *n/a*, 2402467.
[50] R. Jaafar, C. A. Pignedoli, G. Bussi, K. Aït-Mansour, O. Groening, T. Amaya, T. Hirao, R. Fasel, P. Ruffieux, *J. Am. Chem. Soc.* **2014**, *136*, 13666–13671.
[51] L. Gross, F. Mohn, N. Moll, B. Schuler, A. Criado, E. Guitián, D. Peña, A. Gourdon, G. Meyer, *Science* **2012**, *337*, 1326–1329.
[52] P. Hapala, G. Kichin, C. Wagner, F. S. Tautz, R. Temirov, P. Jelínek, *Phys. Rev. B* **2014**, *90*, 085421.
[53] K. Walzer, M. Sternberg, M. Hietschold, *Surf. Sci.* **1998**, *415*, 376–384.
[54] T. Huempfner, F. Sojka, R. Forker, T. Fritz, *Surf. Sci.* **2015**, *639*, 80–88.
[55] N. V. Richardson, in *Surface and Interface Science*, **2016**, pp. 629–693.
[56] M. Lackinger, S. Griessl, W. M. Heckl, M. Hietschold, *J. Phys. Chem. B* **2002**, *106*, 4482–4485.
[57] J. Björk, F. Hanke, S. Stafström, *J. Am. Chem. Soc.* **2013**, *135*, 5768–5775.
[58] C. Sánchez-Sánchez, A. Nicolaï, F. Rossel, J. Cai, J. Liu, X. Feng, K. Müllen, P. Ruffieux, R. Fasel, V. Meunier, *J. Am. Chem. Soc.* **2017**, *139*, 17617–17623.
[59] B. Cirera, N. Giménez-Agulló, J. Björk, F. Martínez-Peña, A. Martin-Jimenez, J. Rodriguez-Fernandez, A. M. Pizarro, R. Otero, J. M. Gallego, P. Ballester, J. R. Galan-Mascaros, D. Ecija, *Nat. Commun.* **2016**, *7*, 11002.
[60] R. Zhang, B. Xia, H. Xu, N. Lin, *Angew. Chem. Int. Ed.* **2019**, *58*, 16485–16489.
[61] C. Zhang, E. Kazuma, Y. Kim, *Angew. Chem. Int. Ed.* **2019**, *58*, 17736–17744.

Manuscript received: August 1, 2024
Accepted manuscript online: August 28, 2024
Version of record online: October 25, 2024